Spatiotemporal stability and control of one-way open coupled Lorenz systems

Keiji Konishi*
Department of Electrical and Electronic Systems, Osaka Prefecture University, 1-1 Gakuen-cho, Sakai, Osaka 599-8531, Japan
(Received 10 April 2001; published 11 February 2002)

We investigate the spatiotemporal stability of a homogeneous solution in one-way open coupled Lorenz systems, and suppress the spatial instability in the systems by using the H_∞ control technique. The suppression is illustrated with numerical simulations. In addition, it is shown that the suppression can be also achieved for one-way ring-type systems.

DOI: 10.1103/PhysRevE.65.036203 PACS number(s): 05.45.Gg, 05.45.Xt, 05.45.Ra, 07.05.Dz

I. INTRODUCTION

The spatial extended systems, which generate complex behavior, have created considerable interest. Among various spatial extended systems, coupled map lattices (CML's) are considered as typical spatial systems [1]. The CML's can be classified into several types according to the connection and the boundary condition; the one-way open CML has been investigated as a simple open flow model [1–6]. The CML has a homogeneous solution corresponding to a laminar flow. Kaneko found that the solution becomes unstable even if all eigenvalues of the Jacobi matrix around the solution are in the unit circle [2]. We refer to this phenomenon as the spatial instability. Yamaguchi investigated this phenomenon in detail and derived the instability condition [6]. In recent years, it was shown that this phenomenon can be clarified by using the H_∞ norm, which plays important roles in the field of robust control theory [7]. This approach was easily extended to continuous-time systems [8,9].

On the other hand, controlling chaos is one of the attractive subjects in the field of nonlinear science [10–16]. The most studies on controlling chaos are based on two major control methods: the Ott-Grebogi-Yorke method [17] and the delayed feedback control (DFC) method [18]. Both of them stabilize the desired unstable periodic orbits embedded within a chaotic attractor only by a small feedback signal. Recently, controlling spatiotemporal chaos in the spatial extended systems, such as partial differential equations, coupled ordinary differential equations, and CML, has gained more and more attention [14,19–22].

The spatial instability in the one-way open CML is similar to a turbulent flow in pipes. Hence, the suppression of the spatial instability corresponds to the maintenance of laminar flow. From an engineering point of view, the suppression would be important for avoiding the harmful turbulence. Very recently, it was shown that the spatial instability in one-way open CML can be suppressed by the decentralized DFC method [23].

The purpose of the present paper is to show that the H_∞ control technique can suppress the spatial instability in *continuous-time* systems. This technique has been used as a major method in the field of robust control theory; therefore, there are several useful software packages which support the analysis and the design of control systems [24–29]. This paper employs the one-way open coupled Lorenz systems [30] as *continuous-time* systems.

The plan of this paper is as follows. In Sec. II, we introduce the one-way open coupled Lorenz systems, and explain the definition of spatiotemporal stability by numerical simulations. In Sec. III, we propose a control scheme which suppresses the spatial instability. Section IV discusses our results. Finally we conclude our work in Sec. V.

II. ONE-WAY OPEN COUPLED LORENZ SYSTEMS

A. Spatiotemporal stability

Let us consider the one-way open coupled Lorenz systems proposed in Ref. [30]:

$$\begin{aligned}
&\dot{\xi}_1(i)=\sigma\{\xi_2(i)-\xi_1(i)\},\\
&\dot{\xi}_2(i)=\gamma\{\varepsilon\xi_1(i-1)+(1-\varepsilon)\xi_1(i)\}-\xi_2(i)-\xi_1(i)\xi_3(i),\\
&\dot{\xi}_3(i)=\xi_1(i)\xi_2(i)-\beta\xi_3(i),
\end{aligned} \tag{1}$$

where $i=1,2,...,N$ is the system number, N represents the size of the coupled systems, $\xi_1(i),\xi_2(i),\ \xi_3(i)\in\mathbf{R}$ are the states of system i, and the parameter $\varepsilon\in[0,1]$ represents the coupling strength. The upper edge is fixed at $\xi_1(0)=\xi_{1f}$, then system (1) has the following homogeneous solution:

$$[\xi_1(i)\quad\xi_2(i)\quad\xi_3(i)]^T=[\xi_{1f}\quad\xi_{2f}\quad\xi_{3f}]^T \tag{2}$$

for all $i=1,2,...,N$. The constant values $\xi_{1f},\xi_{2f},\xi_{3f}$ satisfy

$$\begin{aligned}
&0=\sigma(\xi_{2f}-\xi_{1f}),\\
&0=\gamma\{\varepsilon\xi_{1f}+(1-\varepsilon)\xi_{1f}\}-\xi_{2f}-\xi_{1f}\xi_{3f},\\
&0=\xi_{1f}\xi_{2f}-\beta\xi_{3f},
\end{aligned}$$

and they are the same as the fixed point of the uncoupled (i.e., $\varepsilon=0$) Lorenz system. For $\gamma\leqslant 1$, system (1) has a unique fixed point:

$$[\xi_{1f}\quad\xi_{2f}\quad\xi_{3f}]^T=[0\quad 0\quad 0]^T. \tag{3}$$

For $\gamma\geqslant 1$, fixed point (3), and

$$[\xi_{1f}\quad\xi_{2f}\quad\xi_{3f}]^T=[\pm\sqrt{\beta(\gamma-1)}\quad\pm\sqrt{\beta(\gamma-1)}\quad\gamma-1]^T \tag{4}$$

coexist in system (1) [31].

*Electronic address: konishi@ecs.ees.osakafu-u.ac.jp

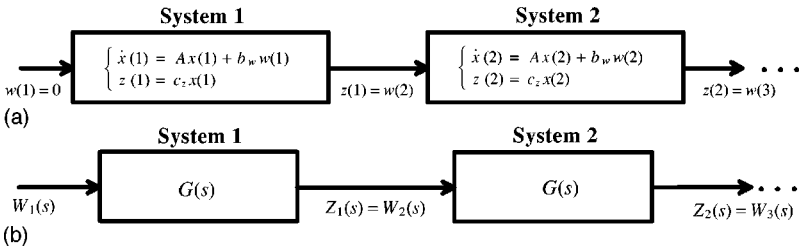

FIG. 1. Linearized system around the homogeneous solution.

The present paper considers the spatiotemporal stability of homogeneous solution (2) on the basis of Ref. [8]. The linearized dynamics around solution (2), illustrated in Fig. 1(a), is described by

$$\begin{aligned} \dot{\mathbf{x}}(i) &= \mathbf{A}\mathbf{x}(i) + \mathbf{b}_w w(i), \\ z(i) &= \mathbf{c}_z \mathbf{x}(i), \end{aligned} \tag{5}$$

where

$$\mathbf{x}(i) = [\xi_1(i) - \xi_{1f} \quad \xi_2(i) - \xi_{2f} \quad \xi_3(i) - \xi_{3f}]^T,$$

$$z(i) = \xi_1(i) - \xi_{1f}, \quad w(i) = \xi_1(i-1) - \xi_{1f},$$

$$\mathbf{A} = \begin{bmatrix} -\sigma & \sigma & 0 \\ \gamma(1-\varepsilon) - \xi_{3f} & -1 & -\xi_{1f} \\ \xi_{2f} & \xi_{1f} & -\beta \end{bmatrix} \tag{6}$$

$$\mathbf{b}_w = [0 \quad \gamma\varepsilon \quad 0]^T, \quad \mathbf{c}_z = [1 \quad 0 \quad 0].$$

The homogeneous solution (2) in system (1) corresponds to $\mathbf{x}(i) = 0$ $(i = 1,2,...,N)$ in the linearized system (5). Hence, in other words, solution (2) is stable if and only if $\lim_{t\to\infty} \mathbf{x}(i) = 0$ for all $i = 1,2,...,N$.

In order to clear the input-output relation, we shall use the frequency domain description of system (5):

$$Z_i(s) = G(s) W_i(s). \tag{7}$$

$Z_i(s)$ and $W_i(s)$ are the Laplace transformations of $z(i)$, $w(i)$, respectively. The transfer function $G(s)$ is given as

$$G(s) = \mathbf{c}_z (s\mathbf{I}_3 - \mathbf{A})^{-1} \mathbf{b}_u, \tag{8}$$

where $\mathbf{I}_3 \in \mathbf{R}^3$ is a unit matrix. Figure 1(b) illustrates system (7).

Now let us assume the ideal situation where there is no external noise in real systems or no round-off-error on computer simulations: $w(1) \equiv 0$ [i.e., $\xi_1(0) \equiv \xi_{1f}$]. If $\mathbf{A}$ is a stable matrix [32], i.e., $G(s)$ is a stable transfer function [33], the system state $\mathbf{x}(1)$ of system 1 will converge on 0. Thus, we have $\lim_{t\to\infty} z(1) = \lim_{t\to\infty} w(2) = 0$ [i.e., $\lim_{t\to\infty} \xi_1(1) = \xi_{1f}$]. We also have the same convergence in lower systems; therefore, the states of all systems behave as $\lim_{t\to\infty} \mathbf{x}(i) = 0$ for all $i = 1,2,...,N$.

In real systems (computer simulations) the states of all systems slightly oscillate around the homogeneous solution (2) due to the external noise (round-off-error). In this case, we should consider an influence of the noise propagation. Reference [8] provided the spatiotemporal stability which takes the noise propagation into account.

Definition 1. The spatiotemporal stability of the homogeneous solution (2) in system (1) is classified into the following three types [8].

(1) If $G(s)$ is unstable, it is temporally unstable (TU).

(2) If $G(s)$ is stable and $\|G(s)\|_\infty < 1$, it is temporally and spatially stable (TSS).

(3) If $G(s)$ is stable and $\|G(s)\|_\infty > 1$, it is temporally stable and spatially unstable (TSSU).

In the field of control theory, it is well known that the H_∞ norm of the transfer function is defined by $\|G(s)\|_\infty := \sup_{\omega\in\mathbf{R}} |G(j\omega)|$. This norm indicates the influence of the input $w(i)$ on the output $z(i)$ in the worst case.

We shall explain the above definition briefly on the basis of Ref. [8]. In the case of TU, each system oscillates due to the unstable transfer function $G(s)$ even if the input signal is fixed at $w(i) \equiv 0$. Thus, none of the systems converge on solution (2). In the case of TSSU, we have an inclination to believe $\lim_{t\to\infty} |z(i)| = 0$ $(i = 1,2,...,N)$, since $G(s)$ is a stable function. However, this is not true. The reason is that the external noise in real systems or the round-off error on computer simulations affects the lower systems. As a result, the states in lower systems cannot stay on solution (2). In the case of TSS, the output signals in lower systems converge on 0 even if the upper systems oscillate with small amplitude.

B. Numerical simulations

We shall confirm our theoretical results by numerical simulations. Throughout this paper we use the standard parameters: $\sigma = 10$ and $\beta = 8/3$. The parameters γ and ε are varied: $1 < \gamma$ and $0 \leqslant \varepsilon \leqslant 1$. We focus on solution (2) consisting of $\xi_{1f} = \sqrt{\beta(\gamma-1)}$, $\xi_{2f} = \sqrt{\beta(\gamma-1)}$, $\xi_{3f} = \gamma - 1$ in Eq. (4). If we consider the other fixed point in Eq. (4), we will have the similar result. In this paper, the well-known Runge-Kutta algorithm with time steps $\Delta t = 0.01$ is used for the numerical integration. The tiny external noise signal is added to the upper edge: $\xi_1(0) = \xi_{1f} + 0.1\rho(n\Delta t)$, where $-1 \leqslant \rho(n\Delta t) \leqslant +1$ is a uniform random value.

First of all, we examine the spatiotemporal stability of homogeneous solution (2) in the Lorenz systems. Figure 2 provides the stability regions on the parameter space $\gamma - \varepsilon$. This figure is obtained by the following procedure: (1) for a parameter set (γ,ε), the transfer function $G(s)$ is derived from Eq. (8); (2) if $G(s)$ is unstable, a dot is plotted at the parameter set as TU and go to Step (5), otherwise go to the next step; (3) if $G(s)$ is stable and $\|G(s)\|_\infty < 1$, a square is plotted as TSS and go to Step (5), otherwise go to the next step; (4) if $G(s)$ is stable and $\|G(s)\|_\infty > 1$, a small dot is plotted as TSSU and go to the next step; (5) the parameter set (γ, ε) is changed to a new parameter set and go back to Step

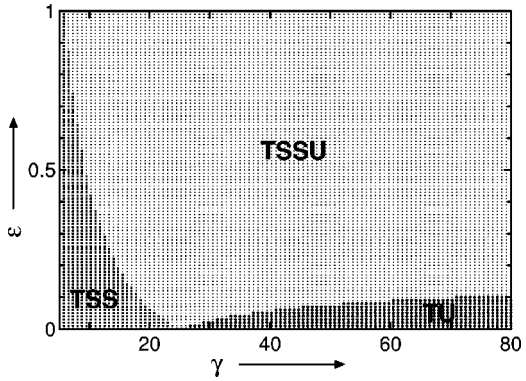

FIG. 2. Spatiotemporal stability of the coupled Lorenz systems.

(1). This procedure can be achieved by a simple program using the software [29]. From Fig. 2, we notice that the large part of the parameter space is occupied by the TSSU region.

The system behavior in the TU region is shown in Fig. 3. The state $\xi_1(1)$ at the upper edge oscillates, and such oscillation is observed in all systems. Now we focus on the TSSU region. The gain $|G(j\omega)|$ is plotted as a function of ω in Fig. 4(a). We notice that the peak gain, i.e., $\|G(s)\|_\infty$, is greater than 1. Hence, the external noise including a frequency bandwidth in which the gain is greater than 1 increases downstream, and then the lower systems oscillate. Figure 4(b) shows the waveforms of the coupled Lorenz systems in the TSSU region. The upper edge system $\xi_1(1)$ has little oscillation; however, the amplitude of oscillations increases downstream. Eventually, we can observe chaotic behavior in the lower systems. Figure 5(a) shows the gain diagram of $G(s)$ in the TSS region. It can be seen that the peak gain is less than 1. The waveforms in the TSS region are shown in Fig. 5(b). It should be noted that the scale of the vertical axis

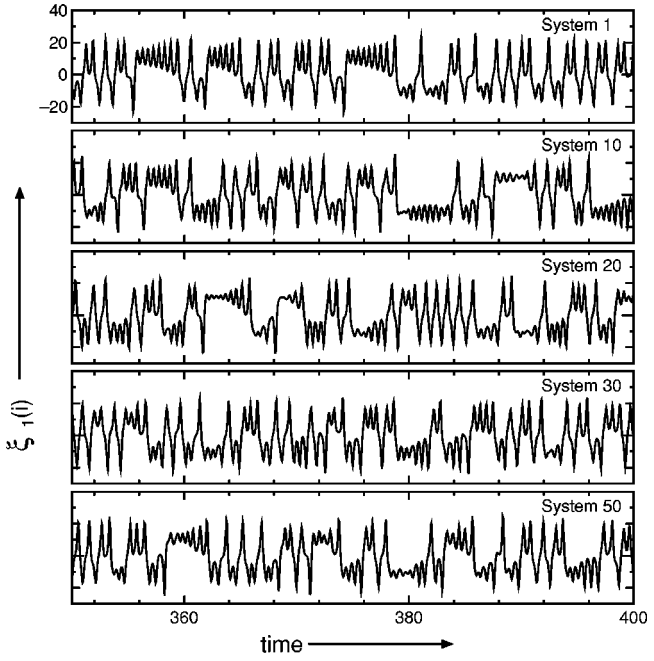

FIG. 3. Waveforms of the coupled Lorenz systems in TU ($\gamma = 50, \varepsilon = 0.05$).

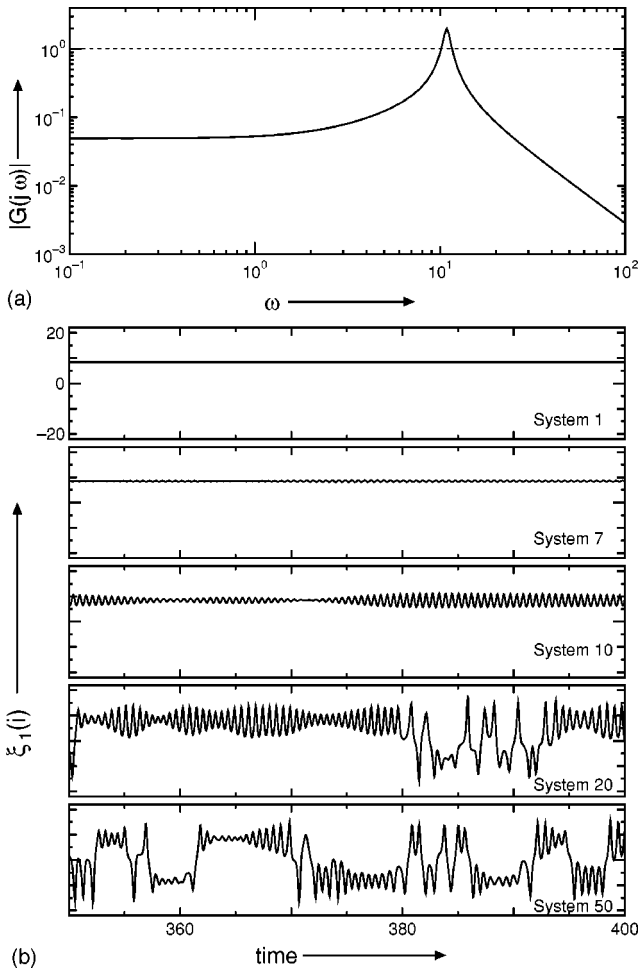

FIG. 4. Gain diagram and waveforms of the coupled Lorenz systems in TSSU ($\gamma = 28, \varepsilon = 0.1$).

in Fig. 5(b) is quite different from Figs. 3 and 4(b). The influence of the upper edge noise decreases downstream. In lower systems we cannot observe the disturbance at all. These numerical results agree well with our theoretical results.

III. SUPPRESSION BY H_∞ CONTROL

Solution (2) in TSSU is similar to a turbulent flow in pipes. The suppression of the spatial instability would be an important subject. This section proposes a control method to convert from the TSSU state (turbulent flow) to the TSS state (laminar flow).

A. Proposal of control system

We propose the control system as shown in Fig. 6(a). This figure describes the only system i; all systems have the same structure. System i is given as

$$\begin{aligned}
\dot{\xi}_1(i) &= \sigma\{\xi_2(i) - \xi_1(i)\} + u(i), \\
\dot{\xi}_2(i) &= \gamma\{\varepsilon\xi_1(i-1) + (1-\varepsilon)\xi_1(i)\} - \xi_2(i) - \xi_1(i)\xi_3(i), \\
\dot{\xi}_3(i) &= \xi_1(i)\xi_2(i) - \beta\xi_3(i).
\end{aligned} \tag{9}$$

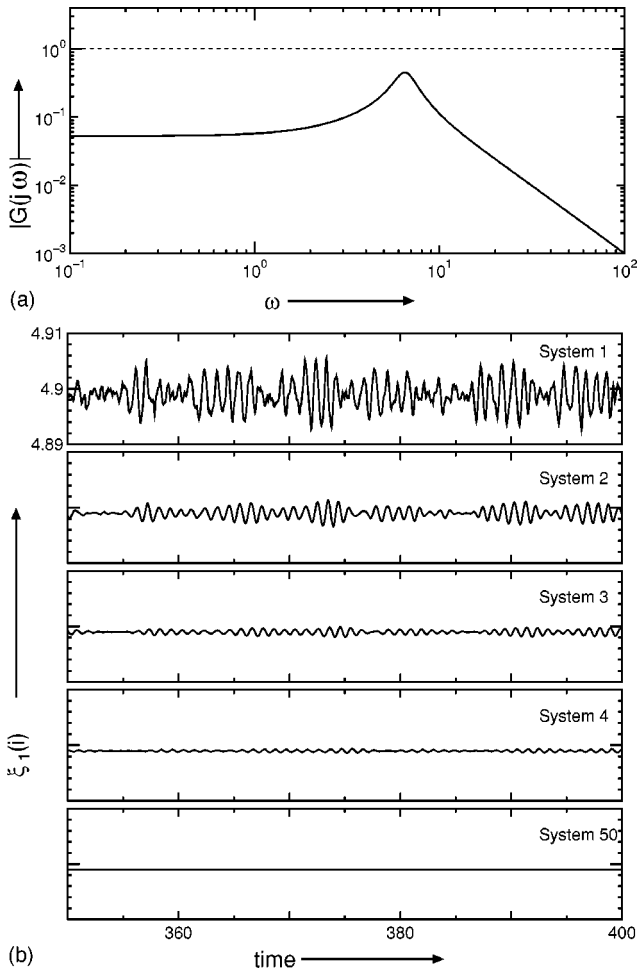

FIG. 5. Gain diagram and waveforms of the coupled Lorenz systems in TSS ($\gamma=10,\varepsilon=0.1$).

$u(i)\in\mathbf{R}$ is the control signal, and the feedback from $\xi_1(i)$ to $u(i)$ is

$$\begin{aligned}\dot{\hat{\mathbf{x}}}(i)&=\mathbf{K}_a\hat{\mathbf{x}}(i)+\mathbf{k}_b y(i),\\ u(i)&=\mathbf{k}_c\hat{\mathbf{x}}(i),\end{aligned}\tag{10}$$

$$y(i)=\begin{cases}\xi_1(i)-\xi_{1f} & d(i)<\nu,\\ 0 & d(i)\geqslant\nu,\end{cases}\tag{11}$$

$$d(i)=\{[\xi_1(i)-\xi_{1f}]^2+[\xi_2(i)-\xi_{2\,f}]^2+[\xi_3(i)-\xi_{3f}]^2\}.$$

$\hat{\mathbf{x}}(i)\in\mathbf{R}^3$ is the state of controller (10) and $\mathbf{K}_a\in\mathbf{R}^{3\times3}$, $\mathbf{k}_b\in\mathbf{R}^{3\times1}$, $\mathbf{k}_c\in\mathbf{R}^{1\times3}$ are the feedback gains we have to determine in advance. Limiter (11) can prevent controller (10) from adding the large signal to the system, since such a signal might make the control system fall into a divergence regime. The threshold $\nu>0$ is set to a small positive value; however, it cannot be designed systematically.

It must be emphasized that solution (2) of coupled system (1) does not change even if controller (10) and limiter (11) are connected to the system. In other words, if the feedback

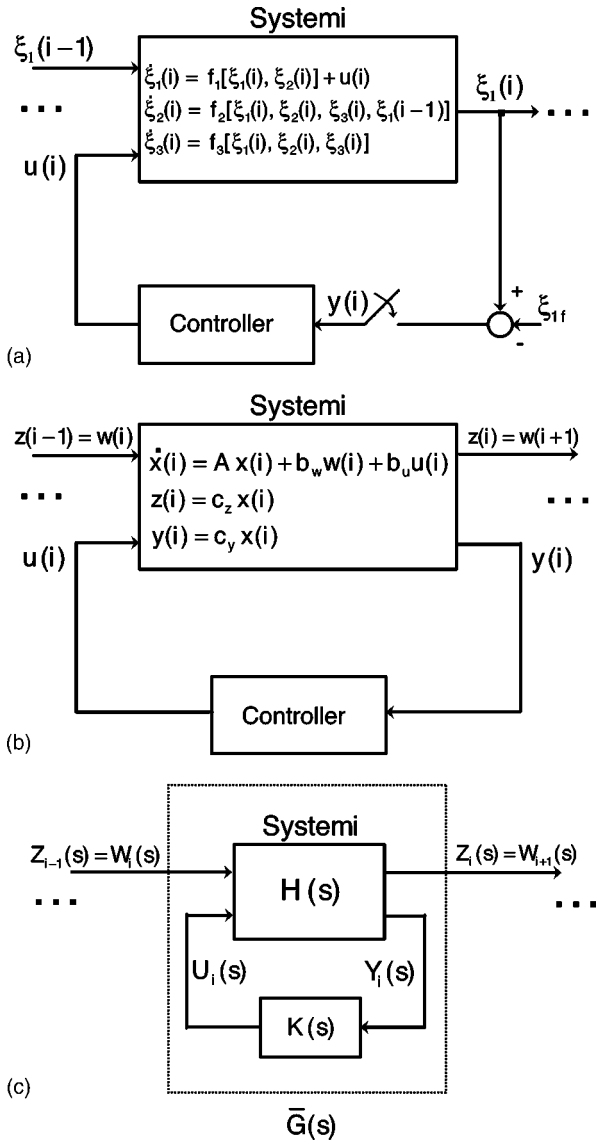

FIG. 6. Proposed system and its linearized system around the homogeneous solution.

gains are suitable, then we can change only the stability of the solution. The linearized system of the controlled Lorenz system (9) around the solution is [see Fig. 6(b)]

$$\begin{aligned}\dot{\mathbf{x}}(i)&=\mathbf{A}\mathbf{x}(i)+\mathbf{b}_w w(i)+\mathbf{b}_u u(i),\\ z(i)&=\mathbf{c}_x\mathbf{x}(i),\\ y(i)&=\mathbf{c}_y\mathbf{x}(i),\end{aligned}\tag{12}$$

for $i=1,2,...,N$, where $\mathbf{b}_u=[1\ 0\ 0]^T$ and $\mathbf{c}_y=[1\ 0\ 0]$. We can transform from the linearized system (12) to the frequency domain description [see Fig. 6(c)]:

$$Z_i(s)=\bar{G}(s)W_i(s).\tag{13}$$

Since system (13) corresponds to system (7), we have to design the feedback gains such that $\bar{G}(s)$ is stable and $\|\bar{G}(s)\|_\infty<1$, where $\bar{G}(s)$ is given by

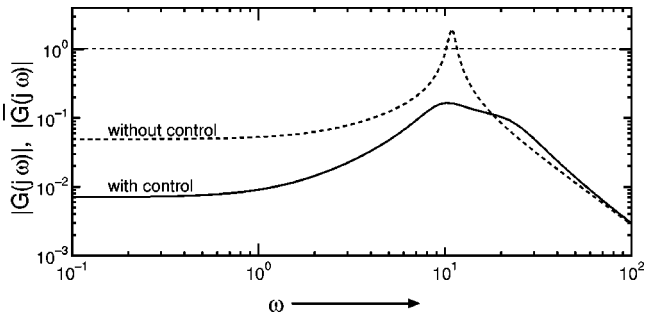

FIG. 7. Gain diagram of the coupled Lorenz system with and without control ($\gamma=28, \varepsilon=0.1$).

$$\overline{G}(s)=H_{11}(s)+H_{12}(s)K(s)[1-H_{22}(s)K(s)]^{-1}H_{21}(s),$$

$$H_{11}(s):=\mathbf{c}_z(s\mathbf{I}-\mathbf{A})^{-1}\mathbf{b}_w, \quad H_{12}(s):=\mathbf{c}_z(s\mathbf{I}-\mathbf{A})^{-1}\mathbf{b}_u,$$

$$H_{21}(s):=\mathbf{c}_y(s\mathbf{I}-\mathbf{A})^{-1}\mathbf{b}_w, \quad H_{22}(s):=\mathbf{c}_y(s\mathbf{I}-\mathbf{A})^{-1}\mathbf{b}_u,$$

$$K(s):=\mathbf{k}_c(s\mathbf{I}-\mathbf{K}_a)^{-1}\mathbf{k}_b.$$

B. Design of controller

Now we provide a problem statement how to design controller (10).

(Design problem). Design the feedback gains $\mathbf{K}_a$, $\mathbf{k}_b$, $\mathbf{k}_c$ such that $\overline{G}(s)$ is stable and $\|\overline{G}(s)\|_\infty<1$.

This is known as the ''suboptimal H_∞ control problem.'' $\overline{G}(s)$ is a transfer function of the closed-loop system consisting of $H(s)$ and $K(s)$ [see Fig. 6(c)]. $\|\overline{G}(s)\|_\infty$ is the H_∞ norm of the transfer function $\overline{G}(s)$, which is the random-mean square gain from $w(i)$ to $z(i)$. This problem seeks a stabilizing controller $K(s)$ that ensures the following: the effect of the worst case disturbance $w(i)$ on the output $z(i)$ will be less than 1. In general, it is difficult to solve this problem theoretically; however, this problem is equivalent to a finding solutions to linear matrix inequalities (LMI's). The solutions to the LMI's form a convex set; therefore, the problem is reduced to a quasiconvex optimization problem which can be solved numerically. In other words, the H_∞ control problem can be solved on computer simulations via LMI formulation. The concrete algorithms for solving this problem is given in Refs. [24–27]. The powerful software [28,29] allows us to obtain the suitable feedback gains by using simple commands. Since the explanation of the LMI-based H_∞ control has no connection with our main subject, we may leave the details to Refs. [28], [29].

C. Numerical simulations

Now we shall try to make a homogeneous solution (2) in the TSSU region be the TSS state. We confirmed on numerical simulations that most of the TSSU region in Fig. 2 can be converted to the TSS region via the LMI-based H_∞ control [34]. As an example, we shall convert the TSSU state in Fig. 4 to the TSS state. The software of the LMI-based H_∞ control provides the following suitable feedback gains [35]:

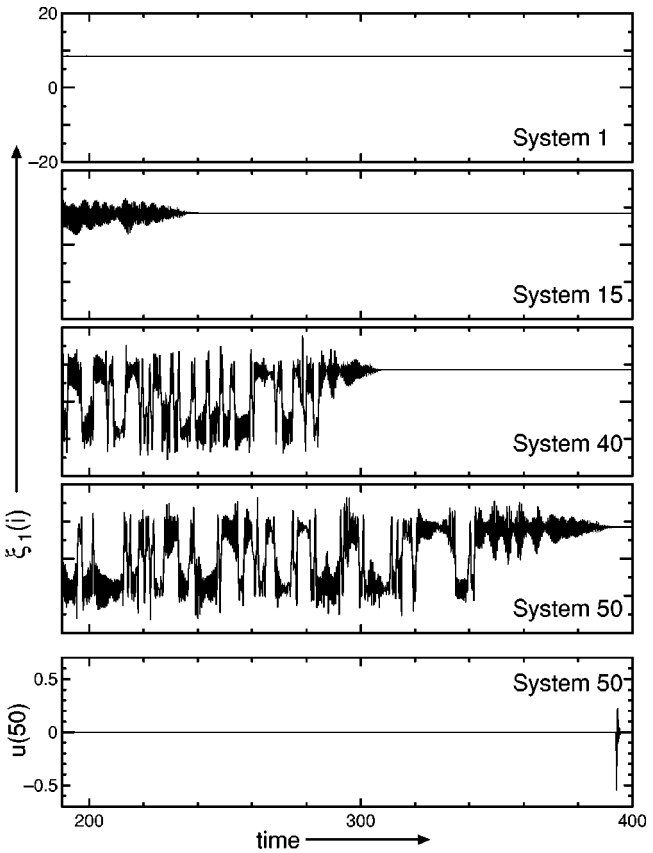

FIG. 8. Waveforms and input signal of the coupled Lorenz systems with control ($\gamma=28, \varepsilon=0.1, \nu=0.1$).

$$\mathbf{K}_a=\begin{bmatrix} -14.500 & -4.933 & 2.198 \\ -9.710 & -4.943 & -8.424 \\ 37.754 & 14.198 & -6.218 \end{bmatrix}$$

$$\mathbf{k}_b=[0.952 \quad 15.791 \quad -38.545]^T,$$

$$\mathbf{k}_c=[-0.789 \quad -3.900 \quad 10.711].$$

The transfer function $\overline{G}(s)$ with the above gains has the poles $[-9.136\pm j21.038, -2.865\pm j9.227, -3.901, -11.423]$; therefore, $\overline{G}(s)$ is a stable matrix. Figure 7 provides the gain diagram. The gain $|G(j\omega)|$ without control has the peak greater than 1; on the contrary, the peak of the gain $|\overline{G}(j\omega)|$ with control is reduced to 0.548. The waveforms and the control signal are shown in Fig. 8. The limiter threshold is set to $\nu=0.1$. The control starts at time $t=200$. We can observe that system states $\xi_1(i)$ $(i=1,2,...,N)$ converge on ξ_{1f} in the order of the system number i. It can be seen that control signal $u(50)$ is within a small range. If the limiter threshold is set to large values, we can observe the following phenomena: the time period for the system convergence becomes short; the control signal becomes large. In other words, our control method has a tradeoff between the convergent time and the size of control signal. The tradeoff is not a particular relation, since there is such a relation in the most of methods for controlling chaos.

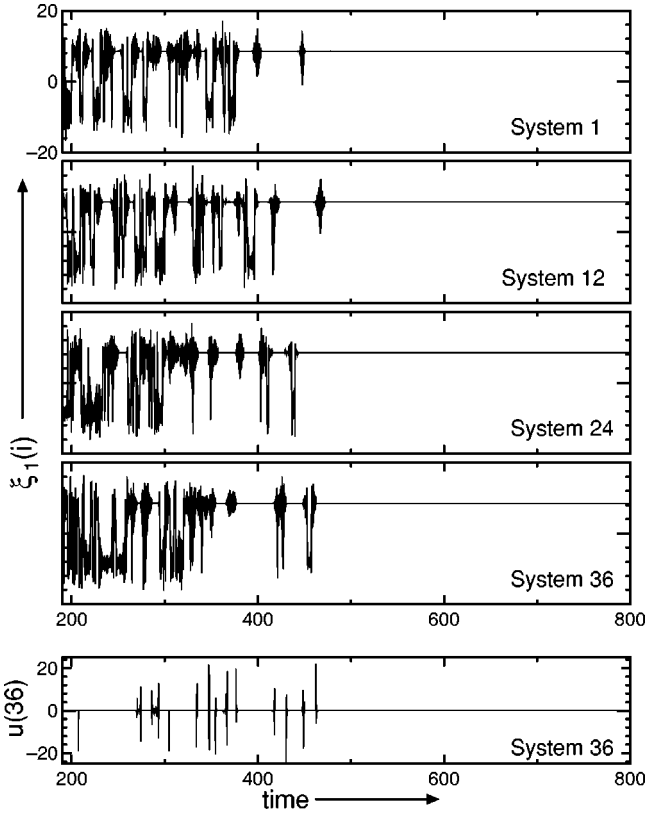

FIG. 9. Waveforms and input signal of the one-way ring coupled Lorenz systems with control ($\gamma=28, \varepsilon=0.1, N=50, \nu=2.5$).

IV. DISCUSSIONS

The above results are for the one-way *open* coupled Lorenz systems. Now, we consider system (1) with $\xi_1(0) \equiv \xi_1(N)$, which describes the one-way *ring* coupled Lorenz systems; the upper edge system is connected to the lower edge one. This section focuses on the ring-type systems on the basis of the above results.

The homogeneous solution (2) in the open-type system (1) is the same as that in the ring-type system. The linearized system around solution (2) in the controlled ring-type system is described by

$$Z_i(s)=\bar{G}(s)Z_{i-1}(s) \quad \text{for} \quad i=1,2,...,N,$$
$$Z_0(s)=Z_N(s). \tag{14}$$

From the small gain theorem [36], the stability condition of system (14) can be simplified as follows: the transfer function $\bar{G}(s)$ is stable and $\|\bar{G}(s)\|_\infty<1$. We notice that this condition is identical to the condition for the open-type systems to be TSS. Therefore, controller (10) designed by the LMI-based approach for the open-type systems can be directly applied to the ring-type systems.

Figure 9 shows the numerical stabilization of the one-way ring coupled Lorenz systems. The parameters and the controller are the same as Fig. 8. We do not add the noise signal to the systems. All systems behave chaotically; this phenomenon is quite different from the TSSU state in the open-type systems. The control starts at $t=200$. The limiter threshold is set to $\nu=2.5$. The bottom of Fig. 9 is the control signal $u(36)$. It can be seen that the amplitude of this signal is large compared with that in Fig. 8 due to the large threshold ν. Unfortunately, we cannot clear the mechanism of the transient behavior in the controlled systems. There is room for further investigation.

V. CONCLUSION

We have shown that the H_∞ control based on the LMI can suppress the spatial instability in the one-way open coupled Lorenz systems. Additionally, we have considered that our approach is also useful for ring-type systems.

This paper has shown only the theoretical and numerical results; therefore, we have to confirm these results by real experimental circuits [9]. Our approach requires the controller whose dimension is the same as the dimension of each system; on the contrary, low dimensional controllers are more desirable from the practical point of view. Therefore, we will have to examine reducing the controller dimension. Furthermore, in our approach, the controller is added to all systems. This is not convenient for practical situations; hence, we plan in the future to discuss the reduction of the controller density.

ACKNOWLEDGMENTS

The author would like to thank Professor H. Kokame and Professor K. Hirata for useful suggestions. The present work was partially supported by the Japan Society for the Promotion of Science (Grant No. 13750430, 2001).

[1] K. Kaneko, Chaos **2**, 279 (1992).
[2] K. Kaneko, Phys. Lett. A **111**, 321 (1985).
[3] R. J. Deissler and K. Kaneko, Phys. Lett. A **119**, 397 (1987).
[4] F. H. Willeboordse, Chaos **2**, 423 (1992).
[5] F. H. Willeboordse and K. Kaneko, Phys. Rev. Lett. **73**, 533 (1994).
[6] A. Yamaguchi, Int. J. Bifurcation Chaos Appl. Sci. Eng. **7**, 1529 (1997).
[7] K. Konishi, H. Kokame, and K. Hirata, Phys. Lett. A **263**, 307 (1999).
[8] K. Konishi, H. Kokame, and K. Hirata, Phys. Rev. E **62**, 6383 (2000).
[9] K. Konishi, H. Kokame, and K. Hirata, IEEE Trans. Circuits Syst. **48**, 1234 (2001).
[10] T. Kapitaniak, *Controlling Chaos* (Academic, New York, 1996).
[11] K. Judd *et al.*, *Control and Chaos* (Birkhauser Boston, Boston, 1997).
[12] G. Chen and X. Dong, *From Chaos to Order* (World Scientific, Singapore, 1998).

[13] A. L. Fradkov and A. Y. Pogromsky, *Introduction to Control of Oscillations and Chaos* (World Scientific, Singapore, 1998).
[14] H. G. Schuster, *Handbook of Chaos Control* (Wiley-VCh, Weinheim, 1999).
[15] G. Chen, *Controlling Chaos and Bifurcations in Engineering Systems* (Chemical Rubber, Boca Raton, FL, 1999).
[16] T. Shinbrot *et al.*, Nature (London) **363**, 411 (1993).
[17] E. Ott, C. Grebogi, and J. A. Yorke, Phys. Rev. Lett. **64**, 1196 (1990).
[18] K. Pyragas, Phys. Lett. A **170**, 421 (1992).
[19] M. Kim *et al.*, Science **292**, 1357 (2001).
[20] S. Dasgupta and D. R. Andersen, J. Opt. Soc. Am. B **11**, 290 (1994).
[21] D. E. Hill *et al.*, IEEE J. Sel. Top. Quantum Electron. **1**, 150 (1995).
[22] D. Auerbach and J. A. Yorke, J. Opt. Soc. Am. B **13**, 2178 (1996).
[23] K. Konishi, H. Kokame, and K. Hirata, Phys. Rev. E **62**, 384 (2000).
[24] P. Gahinet, Int. J. Robust Nonlinear Control **4**, 421 (1994).
[25] P. Gahinet, Automatica **32**, 1007 (1996).
[26] T. Iwasaki and R. E. Skelton, Automatica **30**, 1307 (1994).
[27] S. Boyd *et al.*, *Linear Matrix Inequalities in System and Control Theory* (SIAM, Philadelphia, PA, 1994).
[28] MathWorks, Inc., *Using MATLAB* (MathWorks, Natick, MA, 1996).
[29] P. Gahinet, A. Nemirovski, and A. J. Laub, *LMI Control Toolbox* (MathWorks, Natick, MA, 1995).
[30] M. A. Matias and J. Guemez, Phys. Rev. Lett. **81**, 4124 (1998).
[31] P. Bergé, Y. Pomeau, and C. Vidal, *Order Within Chaos* (Wiley, New York, 1986).
[32] The matrix is stable if and only if each eigenvalue of the matrix has a negative real part.
[33] The transfer function is stable if and only if each pole of the function has a negative real part.
[34] For high-gain feedback, the numerical time steps Δt should be small values (e.g., 0.001 or 0.0001). We also confirm that our control scheme is not valid for some parameter sets. This is because, for the parameter sets, a site behaves oscillatory with a large amplitude even if its upper site is on the fixed point. Our scheme guarantees only the stability in the vicinity of the fixed point; then it is difficult to control the large oscillation.
[35] If we use the optimal algorithm which minimizes $\|\overline{G}(s)\|_\infty$, the feedback gains becomes too large (i.e., high gains). Hence, this paper uses the suboptimal algorithm which designs the feedback gains such that $\|\overline{G}(s)\|_\infty$ is less than 1.
[36] S. P. Bhattacharyya, H. Chapellat, and L. H. Keel, *Robust Control: The Parametric Approach* (Prentice Hall, Englewood Cliffs, NJ, 1995).